Available online at www.sciencedirect.com
SCIENCE DIRECT®
Theoretical and Applied Fracture Mechanics 42 (2004) 303–316
theoretical and applied fracture mechanics
www.elsevier.com/locate/tafmec

A penny-shaped cohesive crack model for material damage

G. Wang, S.F. Li *

Department of Civil and Environmental Engineering, University of California, Berkeley, CA 94720, USA

Available online 5 November 2004

Abstract

A novel micromechanics based damage model is proposed to address failure mechanism of defected solids with randomly distributed penny-shaped cohesive micro-cracks (Barenblatt–Dugdale type). Energy release contribution to the material damage process is estimated in a representative volume element (RVE) under macro hydrostatic stress state. Macro-constitutive relations of RVE are derived via self-consistent homogenization scheme, and they are characterized by effective nonlinear elastic properties and a class of pressure sensitive plasticity which depends on crack opening volume fraction and Poisson's ratio. Several distinguished features of the present model are compared with Gurson model and Gurson–Tvergaard–Needleman (GTN) model, showing that the proposed model can better capture material degradation and catastrophic failure due to cohesive micro-crack growth and coalescence.

Keywords: Cohesive crack model; Damage; Fracture; Micromechanics; Plasticity; Homogenization

1. Introduction

Damage modeling has been an important subject in predicting material degradation and failure. In past decades, numerous constitutive models with evolving damage effects have been proposed for various materials. A large number of them are phenomenological in that damage effects are defined by scalar or tensorial quantities without referring directly to the microstructure of the material. Yet another category of methods use micromechanics to relate material microstructure evolution to its macromechanical behaviors. The popular Gurson model [11,12] and its later extensions [26–29] are such examples. The most distinguished feature of the Gurson model is that its effective constitutive relation at macro-level differs from the constitutive relation at micro-level. Microscopically material's failure mechanism is governed by void growth, while at the macro-level the statistically averaged effective response is characterized as pressure sensitive plasticity which depends on a damage indicator—the volume fraction of the void in a representative volume element (RVE).

* Corresponding author. Tel.: +1 510 642 5362; fax: +1 510 643 8928.
E-mail address: li@ce.berkeley.edu (S.F. Li).

0167-8442/$ - see front matter © 2004 Elsevier Ltd. All rights reserved.
doi:10.1016/j.tafmec.2004.09.005

In principle, a more realistic micromechanics model and a feasible homogenization scheme should lead to a better constitutive law at macro-level. For Gurson model, failure mechanism due to void growth is supported by many experimental observations on failures of ductile materials (e.g. [8,10,20,24,29]). On the other hand, in most brittle, quasi-brittle, and even some ductile materials (such as concrete, rocks, ceramics and some metals), material's failure mechanism may be attributed to propagation, nucleation and coalescence of micro-cracks as well. Although several micro-crack based damage models have been proposed to describe elastic damage processes (e.g. [4,9,15,16,19] and others), few micro-crack damage models are available for inelastic damage processes.

The *motif* of contemporary micromechanics is aimed at discovering unknown but important effective constitutive information by homogenizing massive numbers of micro-objects with simple structures. In this paper, new cohesive damage models are derived based on homogenization of randomly distributed penny-shaped cohesive cracks (Barenblatt–Dugdale type [1,2,7]) in an elastic RVE. At micro-level, the cohesive damage model mimics realistic interactions among atomistic bond forces at crack tips, hence it may capture the overall damage effects due to crack opening and propagation.

In general, damage means material degradation caused by defects or deformation. Damage may be defined as surface separations, permanent lattice distortion, various irreversible effects due to endochronic dissipation etc. In the context of this paper, the term damage is strictly referred to the material degradation due to specific defect—permanent crack opening, or volume fraction of permanent micro-crack opening, which may be viewed as a second phase in a composite material. This definition of damage has been extensively used in engineering literature. The definition of damage used in Gurson model (e.g. void growth) belongs to this category as well.

To distinguish the damage caused by deviatoric stress, such as dislocation, disclination, and surface sliding, with the damage caused by hydrostatic stress, such as permanent crack opening, may simplify constitutive modeling. Of course in reality, material damage may be susceptible and related to both hydrostatic and deviatoric stress states and it is sensitive to their combinations. However, it is a reasonable approximation to assume that the damage due to permanent crack opening is only related to hydrostatic stress state, which renders a tractable homogenization solution.

Throughout this paper, vectors and tensors are denoted as bold-face letters, while their components are written as italic. The symbol '$\cdot$' denotes inner product of two vectors $\mathbf{a}\cdot\mathbf{b}=a_ib_i$ or contraction of adjacent indices of a vector and a tensor (e.g. $\mathbf{n}\cdot\boldsymbol{\sigma}=n_i\sigma_{ij}$). The symbol ':' denotes an inner product of two second-order tensors (e.g. $\mathbf{c}:\mathbf{d}=c_{ij}d_{ij}$) or a double contraction of adjacent indices of tensors of rank two and higher (eg. $\mathbf{C}:\boldsymbol{\varepsilon}=C_{ijkl}\varepsilon_{kl}$).

2. Average theorem for an RVE with cohesive cracks

One of the fundamental concept in classical micromechanics is so called representative volume element (RVE). An RVE for a material point usually contains a very large number of microstructures and it is statistical representative of the local continuum properties. Despite heterogeneity of microstructures, averaged stress or strain properties of an RVE can be derived under specific boundary conditions. For an RVE with randomly distributed cohesive cracks inside, traditional micromechanics averaging theory for traction-free defects [23] cannot be applied. In this section, averaging theorem for RVE containing cohesive defects with constant cohesive traction would be derived for our purpose.

Define the volume average operator $\langle\cdot\rangle$, and define *macro stress tensor* $\boldsymbol{\Sigma}$ as the volume average of micro stress tensor in an RVE,

$$\boldsymbol{\Sigma}=\langle\boldsymbol{\sigma}\rangle=\frac{1}{V}\int_V\boldsymbol{\sigma}\,\mathrm{d}V \tag{1}$$

First, consider the average stress in a three-dimensional elastic RVE with a single penny-shaped Barenblatt–Dugdale crack at the center. Neglect-

ing body force, the equilibrium equation inside an RVE takes the form

$$\nabla \cdot \boldsymbol{\sigma} = 0 \quad \forall \mathbf{x} \in V \tag{2}$$

Assume that the prescribed tractions on the remote boundary of the RVE (∂V_∞) are generated by a constant stress tensor $\boldsymbol{\sigma}^\infty$. Let ∂V_{ec} denote traction-free part of a cohesive crack surface, and let ∂V_{pz} denote the cohesive part of the crack surface where constant traction force $\mathbf{t}$ is applied. Using divergence theorem and Eq. (2), it is straightforward to show that

$$\begin{aligned}\langle \boldsymbol{\sigma} \rangle &= \frac{1}{V}\int_V \boldsymbol{\sigma}\,\mathrm{d}V = \frac{1}{V}\int_V \{\nabla \cdot (\boldsymbol{\sigma} \otimes \mathbf{x})\}^{\mathrm{T}}\,\mathrm{d}V \\ &= \frac{1}{V}\left\{\int_V \boldsymbol{\sigma}^\infty\,\mathrm{d}V - \int_{\partial V_{ec}} \{\mathbf{n} \cdot (\boldsymbol{\sigma} \otimes \mathbf{x})\}^{\mathrm{T}}\,\mathrm{d}S \right. \\ &\quad \left. - \int_{\partial V_{pz}} \{\mathbf{n} \cdot (\boldsymbol{\sigma} \otimes \mathbf{x})\}^{\mathrm{T}}\,\mathrm{d}S\right\} \\ &= \boldsymbol{\sigma}^\infty - \frac{1}{V}\int_{\partial V_{pz}} \{\mathbf{n} \cdot (\boldsymbol{\sigma} \otimes \mathbf{x})\}^{\mathrm{T}}\,\mathrm{d}S \\ &= \boldsymbol{\sigma}^\infty - \frac{1}{V}\int_{\partial V_{pz}} \mathbf{x} \otimes \mathbf{t}\,\mathrm{d}S \end{aligned} \tag{3}$$

where $\mathbf{t}$ is the constant cohesive traction.

Note that $\partial V_{pz} = \partial V_{pz+} \cup \partial V_{pz-}$ and the surface areas $|\partial V_{pz+}| = |\partial V_{pz-}| = \frac{1}{2}|\partial V_{pz}|$, where subscript '+' and '−' are used to distinguish upper and lower part of the crack surfaces. So the last term in Eq. (3) becomes

$$\begin{aligned}\frac{1}{V}\int_{\partial V_{pz}} \mathbf{x} \otimes \mathbf{t}\,\mathrm{d}S &= \frac{1}{V}\left(\int_{\partial V_{pz+}} \mathbf{x} \otimes \mathbf{t}^+\,\mathrm{d}S + \int_{\partial V_{pz-}} \mathbf{x} \otimes \mathbf{t}^-\,\mathrm{d}S\right) \\ &= \frac{1}{2V}\mathbf{x} \otimes (\mathbf{t}^+ + \mathbf{t}^-)\,|\,\partial V_{pz}\,| = 0 \end{aligned} \tag{4}$$

where $\mathbf{t}^+ = -\mathbf{t}^-$ are the cohesive tractions acting on ∂V_{pz+} and ∂V_{pz-} respectively.

Therefore, the average stress inside the RVE will equal to remote stress

$$\boldsymbol{\Sigma} = \langle \boldsymbol{\sigma} \rangle = \boldsymbol{\sigma}^\infty \tag{5}$$

By superposition, it is straightforward to generate this result to an RVE with N cohesive cracks randomly distributed inside (see Fig. 1),

$$\langle \boldsymbol{\sigma} \rangle = \boldsymbol{\sigma}^\infty - \frac{1}{V}\sum_{\alpha=1}^{N}\int_{\partial V_{pz}^{(\alpha)}} \mathbf{x} \otimes \mathbf{t}^{(\alpha)}\,\mathrm{d}S = \boldsymbol{\sigma}^\infty \tag{6}$$

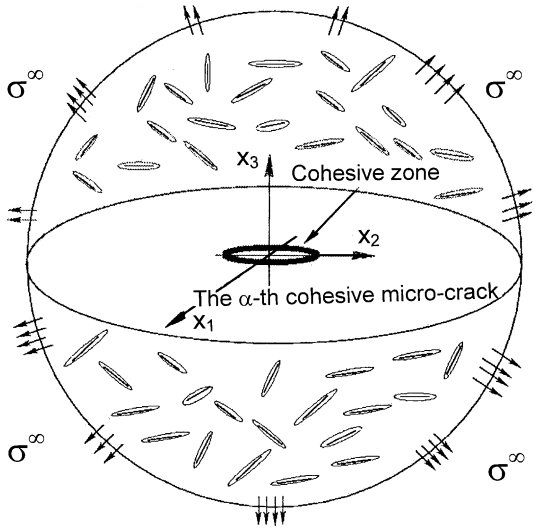

Fig. 1. Randomly distributed micro-cracks within an RVE.

Hence, the averaging theorem follows:

Theorem. *Suppose*

1. *an elastic representative volume element contains N Barenblatt–Dugdale penny-shaped cracks with cohesive tractions in the cohesive zones*;
2. *the tractions on the remote boundary of the RVE is generated by a constant stress tensor, i.e.,* $\mathbf{t}^\infty = \mathbf{n} \cdot \boldsymbol{\sigma}^\infty$ *and* $\boldsymbol{\sigma}^\infty$ *is constant.*

Then, macro stress of the RVE equals to the remote constant stress, i.e. $\boldsymbol{\Sigma} = \langle \boldsymbol{\sigma} \rangle = \boldsymbol{\sigma}^\infty$.

3. Penny-shaped crack under uniform triaxial tension

Before homogenization, the analytical solution of three-dimensional (3D) penny-shaped crack in an RVE that is under uniform triaxial tension is outlined in this section (see Fig. 2).

Penny-shaped Dugdale crack problem has been studied by several authors. The early contribution was made by Keer and Mura, who used the Tresca yield criterion to link the cohesive strength to micro yield stress [17]. In their study, only uniaxial tension loading was considered. More recently,

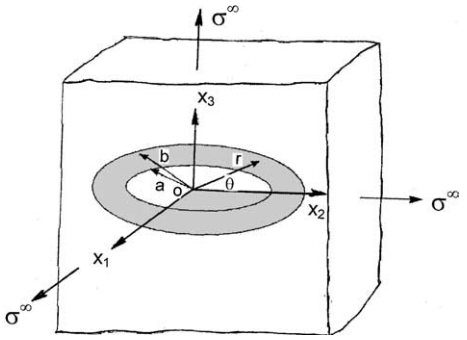

Fig. 2. A penny-shaped cohesive crack in representative volume element (the shaded region: cohesive zone—yielded ring).

Chen and Keer re-examined the problem, and they obtained general solutions for a penny-shaped cohesive crack under mixed-mode loading [5,6]. On the other hand, however, the problem has not been thoroughly examined from micromechanics perspective. For example, the connection among the onset value of cohesive strength, micro yield stress in an RVE, and remote macro stress has not been made. By examining a cohesive penny-shaped crack in an RVE, the study provides a link among cohesive strength, yield stress of virgin material, and remote stresses on the boundary of an RVE, which provides foundation for ensuing homogenizations.

Consider a three-dimensional penny-shaped Dugdale crack of radius a with a ring-shaped cohesive zone with width $b-a$ in an RVE, which may be viewed as an infinite isotropic space by "*a micro-observer*" inside the RVE.

Let the outward normal to crack surface parallel to $Z(X_3)$ axis (see Fig. 2) and uniform triaxial tension stress is applied at the remote boundary of the RVE, i.e.

$$\boldsymbol{\sigma}^{\infty} = \sigma^{\infty}\mathbf{I}^{(2)} \tag{7}$$

where $\mathbf{I}^{(2)} = \delta_{ij}\mathbf{e}_i \otimes \mathbf{e}_j$ is the second-order identity tensor. By the averaging theorem, it is obvious that mean macro stress, defined as $\Sigma_{\mathrm{m}} = \frac{1}{3}\Sigma_{kk}$, equals applied remote stress,

$$\Sigma_{\mathrm{m}} = \sigma^{\infty} \tag{8}$$

In cylindrical coordinate, the traction conditions on the remote boundary ∂V_{∞} and symmetric displacement boundary condition are expressed as

$$\sigma_{zz}|_{\partial V_{\infty}} = \sigma_{\theta\theta}|_{\partial V_{\infty}} = \sigma_{rr}|_{\partial V_{\infty}} = \Sigma_{\mathrm{m}} \tag{9}$$

$$u_z(r,\theta,0) = 0 \quad \text{for } b \leqslant r,\ 0 \leqslant \theta \leqslant 2\pi \tag{10}$$

The stress distribution on the crack surface and cohesive zone is

$$\sigma_{zz}(r,\theta,0) = \sigma_0 H(r-a) \quad \text{for } 0 \leqslant r \leqslant b,\ 0 \leqslant \theta \leqslant 2\pi \tag{11}$$

where Σ_{m} is the remote stress, $H(r-a)$ is the Heaviside function, and σ_0 is the material's cohesive strength, the onset value for crack opening, and it is different from the micro yielding stress. The problem can be solved via superposition of two sub-problems: a trivial problem—an intact RVE in uniform triaxial tension state, i.e. $\forall \mathbf{x} \in V$,

$$\sigma_{zz}^{(0)} = \sigma_{\theta\theta}^{(0)} = \sigma_{rr}^{(0)} = \Sigma_{\mathrm{m}} \tag{12}$$

$$\sigma_{rz}^{(0)} = \sigma_{r\theta}^{(0)} = \sigma_{z\theta}^{(0)} = 0 \tag{13}$$

and a crack problem—an RVE with a center crack that is subjected to the following boundary conditions (see Fig. 3):

$$\sigma_{zz}^{(c)}|_{\partial V_{\infty}} = \sigma_{\theta\theta}^{(c)}|_{\partial V_{\infty}} = \sigma_{rr}^{(c)}|_{\partial V_{\infty}} = 0 \tag{14}$$

$$\sigma_{zz}^{(c)}(r,\theta,0) = -\Sigma_{\mathrm{m}} + \sigma_0 H(r-a) \quad \text{for } 0 \leqslant r \leqslant b,\ 0 \leqslant \theta \leqslant 2\pi \tag{15}$$

$$u_z^{(c)}(r,\theta,0) = 0 \quad \text{for } b \leqslant r,\ 0 \leqslant \theta \leqslant 2\pi \tag{16}$$

For the crack problem, the crack opening displacement could be solved as

$$u_z(r) = \begin{cases} \frac{2}{\pi}\left(\frac{1-v^*}{\mu^*}\right)\left(\Sigma_{\mathrm{m}}\sqrt{b^2-r^2} - \sigma_0\int_a^b \sqrt{t^2-a^2}/\sqrt{t^2-r^2}\,\mathrm{d}t\right), & 0 < r < a \\ \frac{2}{\pi}\left(\frac{1-v^*}{\mu^*}\right)\left(\Sigma_{\mathrm{m}}\sqrt{b^2-r^2} - \sigma_0\int_r^b \sqrt{t^2-a^2}/\sqrt{t^2-r^2}\,\mathrm{d}t\right), & a < r < b \end{cases} \tag{17}$$

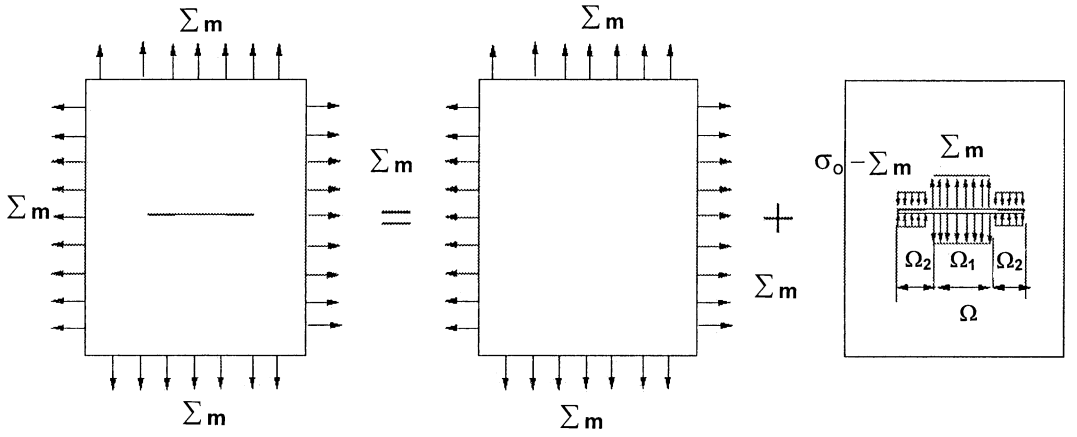

Fig. 3. Illustration of superposition of cohesive crack problem.

In the yield ring ($z = 0$ and $a < r < b$), stress distributions are found as

$$\sigma_{zz}^{(c)} = \sigma_0 - \Sigma_{\mathrm{m}} \tag{18}$$

$$\sigma_{rr}^{(c)} = -\frac{1+2v^*}{2}\Sigma_{\mathrm{m}} + \left[\frac{1-2v^*}{2}\left(1+\frac{a^2}{r^2}\right)+2v^*\right]\sigma_0 \tag{19}$$

$$\sigma_{\theta\theta}^{(c)} = -\frac{1+2v^*}{2}\Sigma_{\mathrm{m}} + \left[\frac{1-2v^*}{2}\left(1-\frac{a^2}{r^2}\right)+2v^*\right]\sigma_0 \tag{20}$$

$$\sigma_{rz}^{(c)} = \sigma_{r\theta}^{(c)} = \sigma_{z\theta}^{(c)} = 0 \tag{21}$$

where Poisson's ratio v^*, to be treated as either overall or matrix material property, is unspecified at this moment, which may depend on the later homogenization procedures.

To ensure the stresses at crack tip to be finite, the size of the cohesive zone a/b, macro stress Σ_{m}, and the cohesive stress σ_0 are related through the following expression:

$$\frac{a}{b} = \sqrt{1-\frac{\Sigma_{\mathrm{m}}^2}{\sigma_0^2}} \quad \text{or} \quad \frac{\Sigma_{\mathrm{m}}}{\sigma_0} = \sqrt{1-\frac{a^2}{b^2}} \tag{22}$$

Denote the projection of traction-free crack surface onto X_1X_2 plane as Ω_1, and the projection of the cohesive zone (ring shape) as Ω_2. The total volume of crack opening by a single cohesive crack is the integration of crack opening displacement

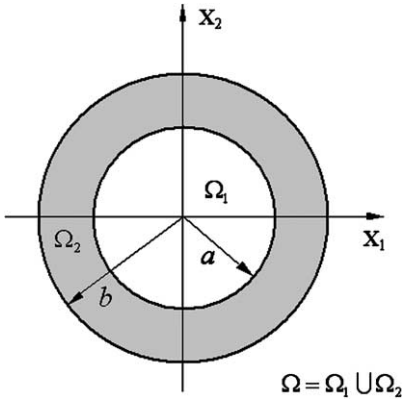

Fig. 4. Projection domain of crack surface and cohesive zone.

over the entire projection area, $\Omega = \Omega_1 \cup \Omega_2$ (see Fig. 4). It is readily to show that

$$\begin{aligned} V_{\mathrm{c}} &= \int_{\Omega}[u_z]\,\mathrm{d}S = \int_{\Omega_1}[u_z]\,\mathrm{d}S + \int_{\Omega_2}[u_z]\,\mathrm{d}S \\ &= \frac{8(1-v^*)}{3\mu^*}b^3\left[\Sigma_{\mathrm{m}} - \sigma_0(1-(a/b)^2)^{3/2}\right] \\ &= \frac{8(1-v^*)}{3\mu^*}a^3\frac{\Sigma_{\mathrm{m}}}{\sqrt{1-(\Sigma_{\mathrm{m}}/\sigma_0)^2}} \end{aligned} \tag{23}$$

where the crack opening displacement, COD, is defined by

$$[u_z] = u_z^+ - u_z^- = 2u_z \tag{24}$$

If one is mainly interested in inelastic deformation of quasi-brittle materials, it may be assumed that

micro-scale yielding due to hydrostatic stress state is small-scale yielding: $\frac{a^2}{b^2} \approx 1$. For $a \leqslant r \leqslant b$, $\frac{a^2}{r^2} \approx 1$. The total stress distribution within cohesive zone ($a \leqslant r \leqslant b$) may be approximated as

$$\sigma_{zz}^{(t)} = \sigma_{zz}^{(0)} + \sigma_{zz}^{(c)} = \sigma_0 \tag{25}$$

$$\sigma_{rr}^{(t)} = \sigma_{rr}^{(0)} + \sigma_{rr}^{(c)} = \frac{1-2v^*}{2}\Sigma_{\mathrm{m}} + \sigma_0 \tag{26}$$

$$\sigma_{\theta\theta}^{(t)} = \sigma_{\theta\theta}^{(0)} + \sigma_{\theta\theta}^{(c)} = \frac{1-2v^*}{2}\Sigma_{\mathrm{m}} + 2v^*\sigma_0 \tag{27}$$

$$\sigma_{rz}^{(t)} = \sigma_{r\theta}^{(t)} = \sigma_{z\theta}^{(t)} = 0 \tag{28}$$

It is assumed that inside the cohesive zone micro plastic yielding is controlled by the Huber–von Mises criterion. Therefore, one can link the cohesive strength, σ_0, with the yield stress of the virgin material, σ_{Y}, by

$$\frac{1}{2}\left[\left(\sigma_{rr}^{(t)} - \sigma_{zz}^{(t)}\right)^2 + \left(\sigma_{\theta\theta}^{(t)} - \sigma_{zz}^{(t)}\right)^2 + \left(\sigma_{rr}^{(t)} - \sigma_{\theta\theta}^{(t)}\right)^2\right] = \sigma_{\mathrm{Y}}^2 \tag{29}$$

Substitute Eqs. (25)–(27) into (29) and solve for σ_0. The following quadratic equation may be obtained:

$$4\left(\frac{\sigma_0}{\Sigma_{\mathrm{m}}}\right)^2 - 2\left(\frac{\sigma_0}{\Sigma_{\mathrm{m}}}\right) + 1 - \left(\frac{2}{1-2v^*}\frac{\sigma_{\mathrm{Y}}}{\Sigma_{\mathrm{m}}}\right)^2 = 0 \tag{30}$$

which has two roots. The positive root is chosen to link the cohesive stress σ_0 with the yield stress σ_{Y} of virgin material in uniaxial tension,

$$\frac{\sigma_0}{\Sigma_{\mathrm{m}}} = \frac{1 + \sqrt{\left(\frac{4}{1-2v^*}\frac{\sigma_{\mathrm{Y}}}{\Sigma_{\mathrm{m}}}\right)^2 - 3}}{4} \tag{31}$$

4. Effective elastic material properties of an RVE

One of the goals of homogenization is to find the effective material properties of an RVE to characterize the constitutive relation of stress and strain relation at the macro-level. Conjugate to the macro stress $\boldsymbol{\Sigma}$, the *macro strain* $\mathbf{E}$ is defined through the overall complementary energy density $\overline{W}_{\mathrm{c}}$ of an RVE

$$\mathbf{E} = \frac{\partial \overline{W}_{\mathrm{c}}}{\partial \boldsymbol{\Sigma}} \tag{32}$$

Define the *effective compliance* $\overline{\mathbf{D}}$ of the micro-cracked RVE through

$$\mathbf{E} = \overline{\mathbf{D}} : \boldsymbol{\Sigma} = \overline{\mathbf{D}} : \boldsymbol{\sigma}^{\infty} \tag{33}$$

where the macro stress $\boldsymbol{\Sigma} = \boldsymbol{\sigma}^{\infty}$, according to average theorem, is regarded as prescribed. It is noted that the macro strain of an RVE may not be the volume average strain, i.e, $\mathbf{E} \neq \langle \boldsymbol{\varepsilon} \rangle$. Furthermore Eq. (33) may not be a linear relationship, because $\overline{\mathbf{D}}$ may depend on $\boldsymbol{\Sigma}$ in general, which will be substantialized in later sections.

A common strategy for homogenization of randomly distributed defects is to divide the macro strain $\mathbf{E}$ into two parts,

$$\mathbf{E} = \boldsymbol{\varepsilon}^{(0)} + \boldsymbol{\varepsilon}^{(a)} \tag{34}$$

where $\boldsymbol{\varepsilon}^{(0)} = \mathbf{D}{:}\boldsymbol{\Sigma}$ is known, and $\mathbf{D}$ is the elastic compliance of the corresponding virgin material. The second term $\boldsymbol{\varepsilon}^{(a)}$ is so-called additional strain tensor representing the effect of defects. If the relationship between additional strain and macro stress can be found, say $\boldsymbol{\varepsilon}^{(a)} = \mathbf{H}{:}\boldsymbol{\Sigma}$, where $\mathbf{H}$ is the added compliance due to micro-cracks, subsequently the effective elastic compliance moduli, $\overline{\mathbf{D}} = \mathbf{D} + \mathbf{H}$, can be deduced.

Energy method is applied to find an additional strain formula for cohesive cracks. The essence of energy methods is to find the energy release in a cohesive fracture process and hence to find the equivalent reduction of material properties. For elastic cracks, the energy release rates were discussed in the classical works of Rice and his co-worker [3,25,26]. Nevertheless, the energy dissipation process of cohesive fracture is much more complicated than a purely elastic fracture process. It includes energy dissipation from both surface separation and plastic dissipation. A related discussion can be also found in [18,22,31].

Although accurate determination of energy loss during a damage process requires an in-depth understanding of the physical process involved, an upper bound estimate may be made based on simplified assumptions. It is assumed that the total energy release of a cohesive crack is completely consumed in surface separation, which may or may not be true in cohesive fracture, because of plastic dissipation in the cohesive zone.

Subjected to uniform triaxial loading $\boldsymbol{\sigma}^{\infty} = \Sigma_{\mathrm{m}}\mathbf{I}^{(2)}$, the total energy release rate of an RVE with a single penny-shaped cohesive micro-crack can be estimated as

$$R = \int_{\Omega} \Sigma_{\mathrm{m}}[u_z]\,\mathrm{d}S - \int_{\Omega_2} \sigma_0[u_z]\,\mathrm{d}S \tag{35}$$

Carrying out the integration using crack displacement solutions Eqs. (17), the energy release estimate can be written as following expression:

$$R = \frac{16(1-v^*)}{3\mu^*}\sigma_0^2 a_\alpha^3\left(1-\sqrt{1-(\Sigma_{\mathrm{m}}/\sigma_0)^2}\right) \tag{36}$$

Consider that there are N penny-shaped cracks inside the RVE. The density of energy release of the RVE is estimated as sum of each crack contribution, i.e. $R = \sum_{\alpha=1}^{N} R_\alpha$. Define the crack opening volume fraction as

$$f = \sum_{\alpha=1}^{N} \frac{4\pi a_\alpha^3}{3V}\beta \tag{37}$$

where a_α is the radius of the αth crack, and $4\pi a_\alpha^3/3$ is the volume of a sphere with radius a_α, and β is the ratio between the volume of permanent crack opening and the volume of total crack opening of a cohesive crack. For simplicity, it is assumed that this ratio is fixed for every crack inside an RVE. Obviously, $0 < \beta < 1$.

By Eqs. (36) and (37), the density of energy release estimate can be written as

$$\begin{aligned}\frac{R}{V} &= \frac{16(1-v^*)}{3\mu^*\beta}\sigma_0^2\sum_{\alpha=1}^{N}\left(\frac{4\pi a_\alpha^3}{3V}\beta\right)\\ &\quad\times\frac{3}{4\pi}\left(1-\sqrt{1-(\Sigma_{\mathrm{m}}/\sigma_0)^2}\right)\\ &= \frac{4(1-v^*)}{\beta\pi\mu^*}\sigma_0^2 f\left(1-\sqrt{1-(\Sigma_{\mathrm{m}}/\sigma_0)^2}\right)\end{aligned} \tag{38}$$

The overall complementary energy density may then be expressed as the sum of complementary energy density of corresponding virgin material and the density of energy release estimate due to micro-crack distribution,

$$\begin{aligned}\overline{W}^c &= W^c + \frac{R}{V} = \frac{1}{2}\boldsymbol{\sigma}^{\infty}:\mathbf{D}:\boldsymbol{\sigma}^{\infty} + \frac{4(1-v^*)}{\beta\pi\mu^*}\sigma_0^2 f\\ &\quad\times\left(1-\sqrt{1-(\Sigma_{\mathrm{m}}/\sigma_0)^2}\right)\end{aligned} \tag{39}$$

Based on definition (32) and the averaging theorem, for a given crack opening volume fraction, f, the elastic macro strain tensor can be obtained as

$$\begin{aligned}\mathbf{E} &= \frac{\partial\overline{W}^c}{\partial\boldsymbol{\Sigma}} = \frac{\partial\overline{W}^c}{\partial\boldsymbol{\sigma}^{\infty}} = \mathbf{D}:\boldsymbol{\sigma}^{\infty} + \frac{\partial(R/V)}{\partial(\Sigma_{\mathrm{m}})}\frac{\partial(\Sigma_{\mathrm{m}})}{\partial\boldsymbol{\sigma}^{\infty}}\\ &= \mathbf{D}:\boldsymbol{\sigma}^{\infty} + \frac{4(1-v^*)}{3\beta\pi\mu^*}f\frac{\Sigma_{\mathrm{m}}\mathbf{I}^{(2)}}{\sqrt{1-(\Sigma_{\mathrm{m}}/\sigma_0)^2}}\end{aligned} \tag{40}$$

It is noted that Eq. (40) holds only when the RVE is under hydrostatic stress state, i.e., $\boldsymbol{\sigma}^{\infty} = \Sigma_{\mathrm{m}}\mathbf{I}^{(2)}$. One can find the expression for additional strain as

$$\boldsymbol{\varepsilon}^{(a)} = \frac{4(1-v^*)}{3\beta\pi\mu^*}f\frac{\Sigma_{\mathrm{m}}\mathbf{I}^{(2)}}{\sqrt{1-(\Sigma_{\mathrm{m}}/\sigma_0)^2}} \tag{41}$$

A bonafide self-consistent scheme should take into account micro-crack interaction (see [4,13,14]). Since the micro-crack distribution is isotropic, the damaged RVE should also be considered as isotropic *at micro-level*. The micro-crack interaction effect could be captured by taking $\mu^* = \bar{\mu}$ and $v^* = \bar{v}$ in all above derivations, where $\bar{\mu}$ and $\bar{v}$ are effective shear modulus and effective Poisson's ratio in an RVE. Recast Eq. (41) into a more general form

$$\boldsymbol{\varepsilon}^{(a)} = \mathbf{H}:\boldsymbol{\Sigma} \tag{42}$$

so

$$\mathbf{E} = \overline{\mathbf{D}}:\boldsymbol{\Sigma} = (\mathbf{D}+\mathbf{H}):\boldsymbol{\Sigma} \tag{43}$$

where $\mathbf{H}$ is an isotropic tensor, which may be written in a general form as

$$\mathbf{H} = \frac{h_1}{3}\mathbf{I}^{(2)}\otimes\mathbf{I}^{(2)} + h_2\mathbf{I}^{(4s)} \tag{44}$$

where $\mathbf{I}^{(2)} = \delta_{ij}\mathbf{e}_i\otimes\mathbf{e}_j$ and

$\mathbf{I}^{(4s)} = \frac{1}{2}(\delta_{ik}\delta_{jl} + \delta_{il}\delta_{jk})\mathbf{e}_i\otimes\mathbf{e}_j\otimes\mathbf{e}_k\otimes\mathbf{e}_l$

are second- and fourth-order identity tensors respectively. Parameters h_1 and h_2 will be specified later.

Decompose the moduli into volumetric and deviatoric parts

$$\mathbf{D} = \frac{1}{3K}\mathbf{E}^1 + \frac{1}{2\mu}\mathbf{E}^2 \tag{45}$$

$$\overline{\mathbf{D}} = \frac{1}{3\overline{K}}\mathbf{E}^1 + \frac{1}{2\bar{\mu}}\mathbf{E}^2 \tag{46}$$

$$\mathbf{H} = (h_1 + h_2)\mathbf{E}^1 + h_2\mathbf{E}^2 \tag{47}$$

where $\mathbf{E}^1 = \frac{1}{3}\mathbf{I}^{(2)} \otimes \mathbf{I}^{(2)}$, $\mathbf{E}^2 = -\frac{1}{3}\mathbf{I}^{(2)} \otimes \mathbf{I}^{(2)} + \mathbf{I}^{(4s)}$.

Since the traction stress state on the remote boundary of the RVE is hydrostatic, $\mathbf{H}$ tensor in Eq. (44) cannot be uniquely determined in this case. Information carried in Eq. (43) is only volumetric and admits only one scalar relation,

$$\overline{\mathbf{D}} : \Sigma_{\mathrm{m}}\mathbf{I}^{(2)} = (\mathbf{D} + \mathbf{H}) : \Sigma_{\mathrm{m}}\mathbf{I}^{(2)} \tag{48}$$

Consider Eq. (34) and identities $\mathbf{E}^1 : \mathbf{I}^{(2)} = \mathbf{I}^{(2)}$ and $\mathbf{E}^2 : \mathbf{I}^{(2)} = 0$. By virtue of Eqs. (41) and (48), it can be shown that

$$\begin{aligned}\frac{1}{3\overline{K}} &= \frac{1}{3K} + (h_1 + h_2) \\ &= \frac{1}{3K} + \frac{4(1-\bar{v})}{3\beta\pi\bar{\mu}} \frac{f}{\sqrt{1 - (\Sigma_{\mathrm{m}}/\sigma_0)^2}}\end{aligned} \tag{49}$$

There are two unknowns, $\overline{K}$ and $\bar{\mu}$, or equivalently h_1 and h_2 in Eq. (49). Additional condition is needed to uniquely determine $\overline{\mathbf{D}}$ or $\mathbf{H}$. Impose the restriction that the relative reduction of the shear modulus is the same as that of the bulk modulus,

$$\frac{\overline{K}}{K} = \frac{\bar{\mu}}{\mu} \tag{50}$$

This restriction further guarantees the positive definiteness of the overall strain energy.

Consider the relations

$$\begin{aligned}\frac{1}{3K} &= \frac{1-2v}{E} \quad \text{and} \quad \frac{1}{3\overline{K}} = \frac{1-2\bar{v}}{\overline{E}} \\ \frac{1}{2\mu} &= \frac{1+v}{E} \quad \text{and} \quad \frac{1}{2\bar{\mu}} = \frac{1+\bar{v}}{\overline{E}}\end{aligned} \tag{51}$$

A direct consequence of Eq. (50) is $\bar{v} = v$, so

$$\begin{aligned}\frac{1}{3\overline{K}} &= \frac{1}{2\bar{\mu}}\left(\frac{1-2\bar{v}}{1+\bar{v}}\right) = \frac{1}{2\bar{\mu}}\left(\frac{1-2v}{1+v}\right) \\ \frac{1}{3K} &= \frac{1}{2\mu}\left(\frac{1-2v}{1+v}\right)\end{aligned} \tag{52}$$

which, when substituted into Eq. (49), leads to the estimates of effective elastic moduli

$$\frac{\overline{K}}{K} = \frac{\bar{\mu}}{\mu} = 1 - \frac{8(1-v^2)}{3\beta\pi(1-2v)} \frac{f}{\sqrt{1 - (\Sigma_{\mathrm{m}}/\sigma_0)^2}} \tag{53}$$

5. Micro-cohesive-crack damage model

Homogenization of nonlinear problems is often difficult. Without proper statistical closure, averaging along may not be sufficient to provide sensible results. In this paper, it is postulated that there is a limit for the amount of distortional energy that a given material ensemble can store. This reflects in the following hypothesis on the condition of macro-yielding:

The macroscopic yielding of an RVE begins when the distortional strain energy density of an RVE reaches to a threshold. In other words, the maximum elastic distortional energy of an RVE is a material constant,

$$U_d \leqslant U_d^{\mathrm{cr}} \tag{54}$$

It is noted that above criterion is a reminiscence of the Hencky's maximum distortional energy principle in traditional infinitesimal plasticity. The criterion can be calibrated using an uniaxial tension test of the virgin material

$$U_d^{\mathrm{cr}} = \frac{1}{6\mu}\sigma_{\mathrm{Y}}^2 \tag{55}$$

Define the macro deviatoric stress tensor and its second invariant as

$$\mathbf{\Sigma}' = \mathbf{\Sigma} - \tfrac{1}{3}\Sigma_{kk}\mathbf{I}^{(2)} \tag{56}$$

$$J_2 = \tfrac{1}{2}\mathbf{\Sigma}' : \mathbf{\Sigma}' \tag{57}$$

and the equivalent macro stress Σ_{eq} is defined as

$$\Sigma_{\mathrm{eq}} = \sqrt{3J_2} \tag{58}$$

In a real damage evolution process, the above criteria take the following form:

$$U_d = \frac{J_2}{2\bar{\mu}} = \frac{\Sigma_{\mathrm{eq}}^2}{6\bar{\mu}} \leqslant U_d^{\mathrm{cr}} \tag{59}$$

So the criterion of the maximum distortional energy density of an RVE becomes

$$\frac{\Sigma_{\mathrm{eq}}^2}{\sigma_{\mathrm{Y}}^2} = \frac{\bar{\mu}}{\mu} \tag{60}$$

Using Eq. (53), one may derive the following effective yielding potential:

$$\Psi(\Sigma_{\mathrm{eq}},\Sigma_{\mathrm{m}},\mathbf{q})=\frac{\Sigma_{\mathrm{eq}}^2}{\sigma_{\mathrm{Y}}^2}+\frac{8(1-v^2)}{3\beta\pi(1-2v)}\times\frac{f}{\sqrt{1-(\Sigma_{\mathrm{m}}/\sigma_0)^2}}-1=0 \tag{61}$$

where Σ_{eq} and Σ_{m} are defined as the equivalent macro stress and mean macro stress, and $\mathbf{q}$ represents the other internal variables, which may be implicitly embedded in σ_{Y}.

In terms of the stress ratio $\Sigma_{\mathrm{m}}/\sigma_{\mathrm{Y}}$, the effective yielding potential function of plastic flow Ψ can be recast as

$$\Psi(\Sigma_{\mathrm{eq}},\Sigma_{\mathrm{m}},\mathbf{q})=\frac{\Sigma_{\mathrm{eq}}^2}{\sigma_{\mathrm{Y}}^2}+\frac{8(1-v^2)f}{3\beta\pi(1-2v)}\times\frac{1+\sqrt{\left(\frac{4\sigma_{\mathrm{Y}}}{(1-2v)\Sigma_{\mathrm{m}}}\right)^2-3}}{\left(\left(1+\sqrt{\left(\frac{4\sigma_{\mathrm{Y}}}{(1-2v)\Sigma_{\mathrm{m}}}\right)^2-3}\right)^2-16\right)^{\frac{1}{2}}}-1=0 \tag{62}$$

The newly derived pressure-sensitive yielding function Ψ, is displayed in Fig. 5 with different Poisson's ratios. It should be mentioned that the self-consistent scheme based damage model Ψ will fail at $v=0.5$, since for incompressible materials, uniform triaxial tension load will not be able to produce dilatational strain energy.

In Fig. 6, the cohesive damage model is juxtaposed with the popular Gurson model [12], whose effective yield function takes the following form:

$$\Phi=\frac{\Sigma_{\mathrm{eq}}^2}{\sigma_{\mathrm{Y}}^2}+2f\cosh\left(\frac{3}{2}\frac{\Sigma_{\mathrm{m}}}{\sigma_{\mathrm{Y}}}\right)-(1+f^2)=0 \tag{63}$$

Both yield functions will reduce to classical J_2 plasticity when $f=0$. However, it is worth noticing that for the limit case of infinitesimal amount of damage (i.e. $f\to 0$), the proposed cohesive damage model predicts yielding of material when the stress ratio of hydrostatic stress and the cohesive strength, or equivalently the ratio of hydrostatic stress and true yield stress, approaches a finite value, i.e.

$$\frac{\Sigma_{\mathrm{m}}}{\sigma_0}\to 1 \quad \text{or} \quad \frac{\Sigma_{\mathrm{m}}}{\sigma_{\mathrm{Y}}}\to\frac{4}{\sqrt{12}(1-2v)} \tag{64}$$

For Gurson model, when the amount of damage is infinitesimal the material will not yield unless the hydrostatic stress becomes infinite. The asymptotic yielding potentials for infinitesimal damage are highlighted as dashed lines in Fig. 6(c) and (d). Obviously, the Gurson model is not realistic, because any material will fail when the remote load exceeds the material's theoretical strength.

In the followings, features of the present model will be explored in the framework of continuum mechanics. The macro response the reversible part of effective constitutive relation is characterized as a nonlinear elasticity, whereas the irreversible part of effective constitutive relation is a form of pressure-sensitive plasticity. The rate form of constitutive relation for damaged materials is written as

$$\dot{\mathbf{\Sigma}}=\overline{\mathbf{C}}:(\dot{\mathbf{E}}-\dot{\mathbf{E}}^{\mathrm{p}}) \tag{65}$$

where $\overline{\mathbf{C}}$ is the effective elastic moduli and $\overline{\mathbf{C}}=\overline{\mathbf{D}}^{-1}$; $\dot{\mathbf{E}}$ and $\dot{\mathbf{E}}^{\mathrm{p}}$ are the average rate of total deformation and the average rate of plastic deformation respectively.

The macro plastic flow direction may be given by the associative rule

$$\dot{\mathbf{E}}^{\mathrm{p}}=\dot{\lambda}\mathbf{N} \tag{66}$$

where $\mathbf{N}$ is the normal of yield surface in stress space

$$\mathbf{N}=\frac{\partial\Psi}{\partial\mathbf{\Sigma}} \tag{67}$$

and the plastic multiplier $\dot{\lambda}$ can be determined by consistency condition as usual,

$$\dot{\lambda}=\frac{\langle\mathbf{N}:\overline{\mathbf{C}}:\dot{\mathbf{E}}\rangle}{\mathbf{N}:\overline{\mathbf{C}}:\mathbf{N}-\Psi_{\mathbf{q}}\cdot\mathbf{N}} \tag{68}$$

where $\Psi_{\mathbf{q}}=\frac{\partial\Psi}{\partial\mathbf{q}}$, $\langle\cdot\rangle$is the Macauley bracket, and $\mathbf{q}$ are internal variables whose evolutions are assumed to be governed by

$$\dot{\mathbf{q}}=\dot{\lambda}\mathbf{h}(\mathbf{\Sigma},\mathbf{q}) \tag{69}$$

The damage evolution law for micro-cracks in a cohesive elastic environment may be significantly different from that of voids in a perfectly viscoplastic environment. For this moment, conventional

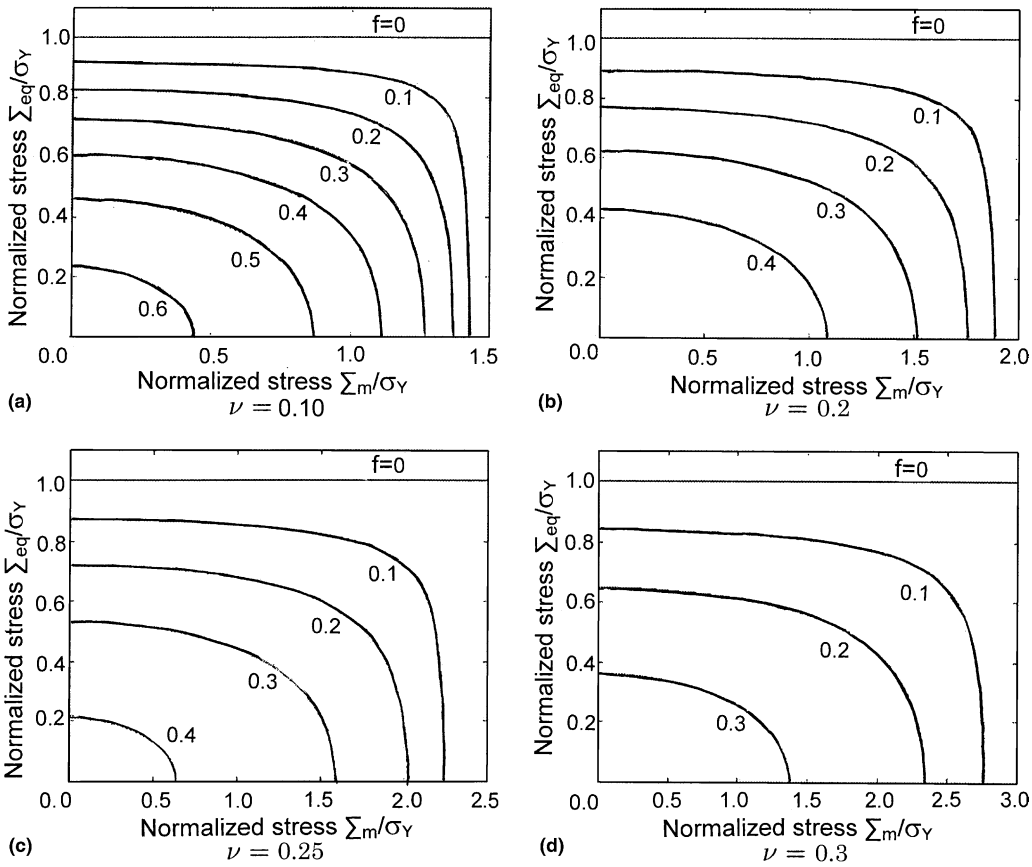

Fig. 5. Cohesive micro-crack damage model, $\Psi(\Sigma_{eq}, \Sigma_m, \mathbf{q})$, with different Poisson's ratios ($\beta = 1/3$).

damage evolution law is adopted. Let the volume of the RVE be denoted as $V = V_m + V_c$, where V_c is the crack opening volume and V_m is the volume of matrix. Assuming the total rate change of the crack volume is proportional to *the volume rate change in an RVE*, i.e.

$$\dot{V}_c = \gamma \dot{V} \tag{70}$$

where γ is the proportionality constant. Then

$$\dot{f} = \frac{d}{dt}\left(\frac{V_c}{V}\right) = (\gamma - f)\frac{\dot{V}}{V} = (\gamma - f)\mathrm{trace}(\dot{\mathbf{E}}) \tag{71}$$

Assume a specimen is originally intact (i.e. $f = 0$), and it is subjected to an uniaxial tension test under displacement control. The onset of material damage, which is physically initiation and propagation of micro-cohesive-cracks, will occur after the specimen first reaches its yield limit (σ_Y, ε_Y).

Let σ and ε denote *axial stress* and *axial strain* of the specimen, it is obvious that $\Sigma_{eq} = \sigma$, $\Sigma_m = \sigma/3$ and $\mathrm{trace}(\dot{\mathbf{E}}) = (1 - 2v)\dot{\varepsilon}$. Eq. (71) is used to describe post-elastic damage evolution process, and for the purpose of illustration one can simply choose $\gamma = 1$. Integrate the rate form, volume fraction f could therefore be deduced from a given axial strain ε,

$$f = 1 - \frac{1}{\exp((1 - 2v)(\varepsilon - \varepsilon_Y))} \tag{72}$$

The corresponding axial stress during persistent plastic loading could be derived via solving yielding potential functions $\Psi(\sigma, \varepsilon) = 0$ or $\Phi(\sigma, \varepsilon) = 0$.

In Figs. 7 and 8, the predicted post-elastic material behaviors of the present model and Gurson model are plotted for various Poisson's ratios. For clarity, initial yield strain ε_Y is neglected in

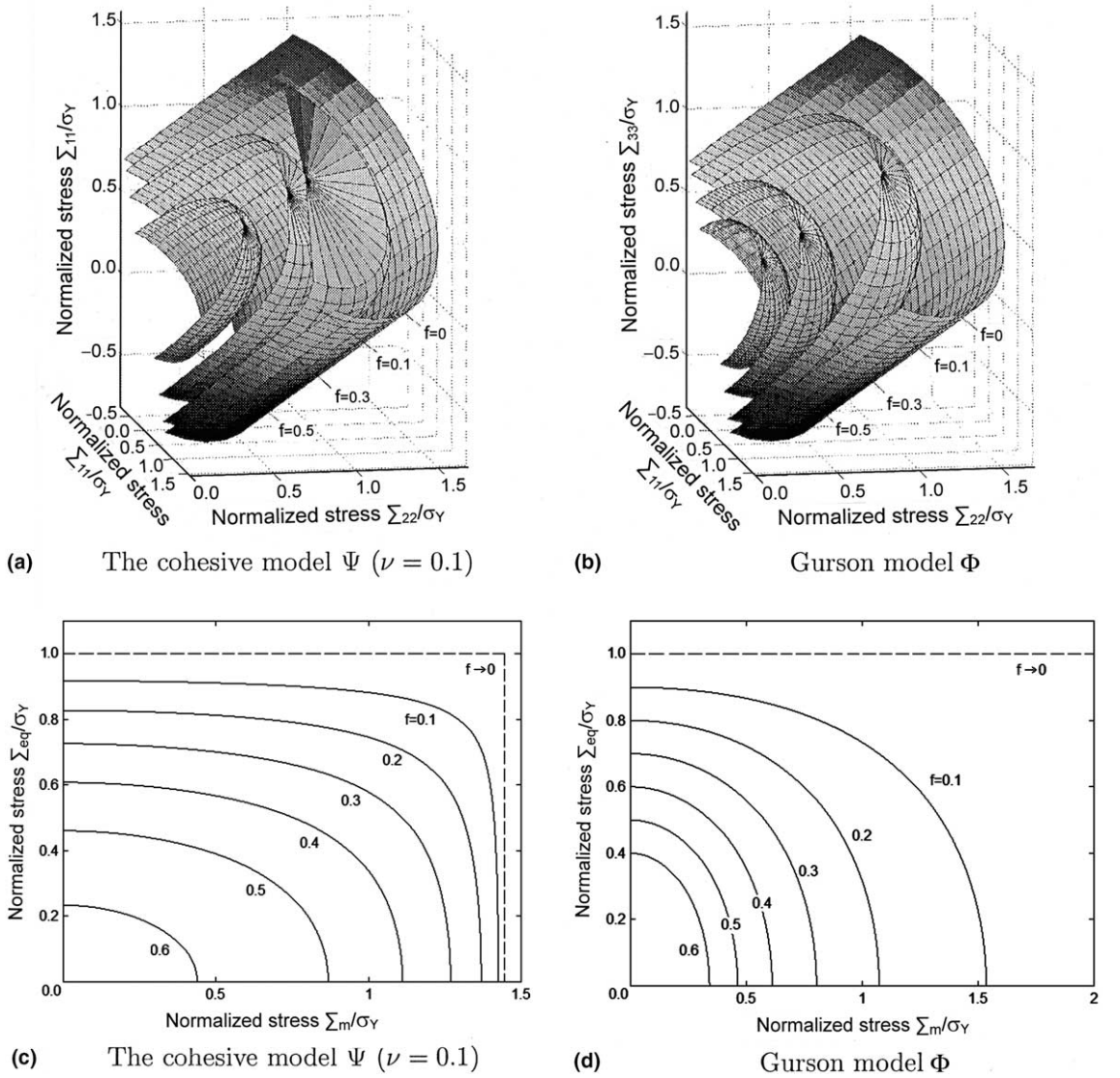

Fig. 6. Comparison between cohesive model Ψ and Gurson model Φ.

all plots. Significant differences between these models solely stem from use of different yield potentials. It is shown that for all Poisson's ratios, the present cohesive crack model predicts similarly quasi-linear degradation at initial stage. As damage develops, specimen collapses catastrophically at a certain strain limit. In another word, the model is able to *predict* a critical volume fraction f_f at which complete failure of material would occur. The predicted f_f for different Poisson's ratio is summarized in Table 1.

It is well known, also as shown in Fig. 8, Gurson model has limitation unable to capture this catastrophic failure. As a sharp contrast, Gurson model predicts quite gentle softening responses. It is also worth mentioning that, as material approaches incompressible limit, i.e. Poisson's ratio is very close to 0.5 ($v = 0.499$ in Figs. 7 and 8),

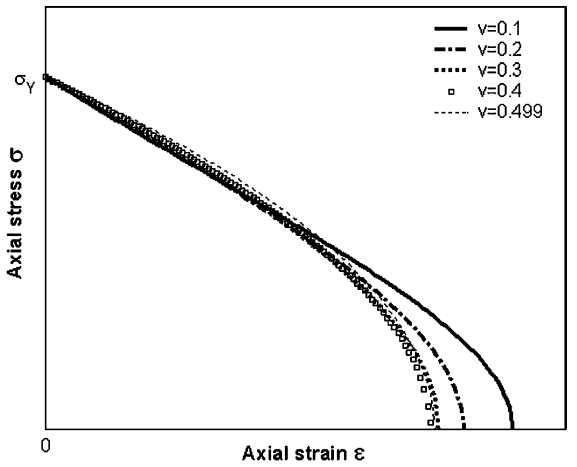

Fig. 7. Cohesive model prediction of axial stress and strain for different Poisson's ratios.

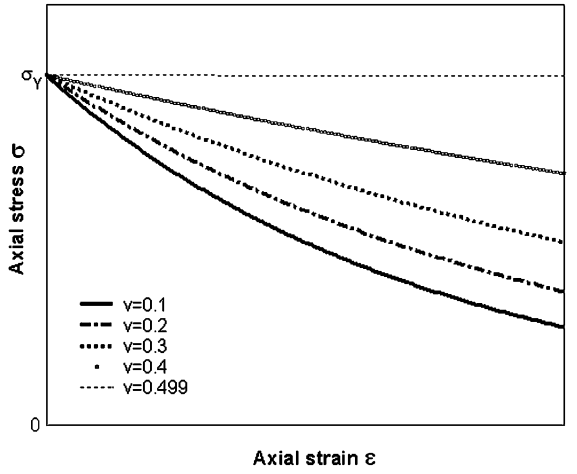

Fig. 8. Gurson model prediction of axial stress and strain for different Poisson's ratios.

Table 1
Predicted critical volume fraction for different Poisson's ratios

v	0.100	0.200	0.300	0.400	0.499
f_f	0.632	0.489	0.343	0.186	0.002

volume fraction change throughout the tension test is very tinny according to Eq. (72). Gurson model reduces to J_2 plasticity and fail to predict any damage effect. While for the present model, because yielding potentials also depend on Poisson's ratio, it is still able to capture softening behavior at the nearly incompressible limit.

To account for the rapid void coalescence at failure, Tvergaard and Needleman extended original Gurson model by introducing parameters q_1, q_2 and f^*. As a modification of Eq. (63), the yielding potential function of Gurson–Tvergaard–Needleman (GTN) model [30] is written as

$$\Phi^* = \frac{\Sigma_{\text{eq}}^2}{\sigma_Y^2} + 2q_1 f^* \cosh\left(\frac{3q_2}{2}\frac{\Sigma_m}{\sigma_Y}\right) - (1 + q_1^2 f^{*2}) = 0 \tag{73}$$

where f^* is specified as a piecewise function of f via

$$f^* = \begin{cases} f & \text{for } f \leqslant f_c \\ f_c + \dfrac{1/q_1 - f_c}{f_f - f_c}(f - f_c) & \text{for } f_c < f \leqslant f_f \\ 1/q_1 & \text{for } f_f < f \end{cases} \tag{74}$$

Note that f_c and f_f are volume fractions at onset of void coalescence and total failure respectively. They are regarded as material constant and need to be specified. It is seen that as volume fraction f grows towards its failure value f_f and f^* approaches $1/q_1$ the yield surface for macro stresses shrinks to a point, so material is "preprogrammed" to fail at $f = f_f$. So in GTN model, effects of void coalescence and total failure are addressed by scaling and interpolation, while failure prediction is embedded in the cohesive cracked model.

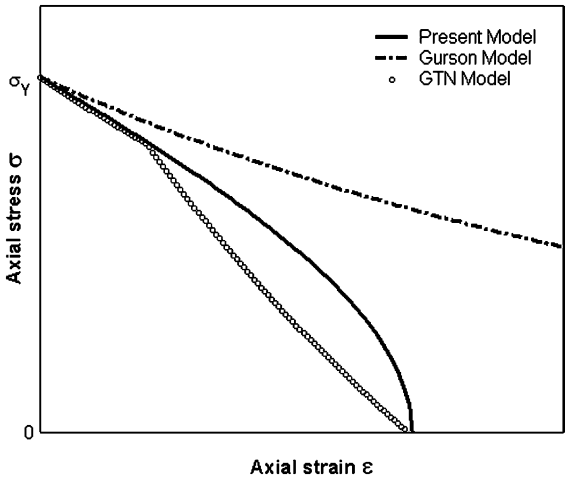

Fig. 9. Comparison of model predictions ($v = 0.3$).

Predictions of all three models are plotted in Fig. 9 for Poisson's ratio $v = 0.3$. For simply illustrative purpose, parameters for GTN model are chosen as $q_1 = 1.5$, $q_2 = 1$, and $f_f = 0.343$, $f_c = f_f/3$. It is noted that above f_f value is chosen on purposely to be the same as that *predicted* by cohesive crack model. Although GTN matches cohesive model at both ends (of course), its undergoes an abrupt change once f exceeds f_c. Damage process towards failure is piecewise quasi-linear and catastrophic failure effect is still absent.

6. Concluding remarks

In this paper, a novel micromechanics based damage model is proposed for addressing failure mechanism of defected solids with randomly distributed penny-shaped cohesive micro-cracks (Barenblatt–Dugdale type). The distinguished features of the present cohesive crack damage models are:

- Homogenized macro-constitutive relations are different from the micro-constitutive relations: the reversible part of macro-constitutive relation is nonlinear elastic versus the linear elastic behaviors at micro-level; the irreversible part of macro-constitutive relation is a form of pressure sensitive plasticity versus the Huber–von Mises plasticity or cohesive laws at micro-level.
- In cohesive damage models, the effective yield surfaces depend on materials Poisson's ratio; whereas in the Gurson model, no such dependence can be predicted, because of its assumption of RVE is perfectly plastic. Different asymptotic yield surfaces are also observed for the case of infinitesimal damage.
- Comparison of the present model with Gurson model and Gurson–Tvergaard–Needleman (GTN) model for a simple loading shows that, the present model can predict a critical volume fraction at which complete failure of material would occur. It can model and predict post elastic material degradation and catastrophic failure due to cohesive micro-crack growth and coalescence.

The key step in the model development is how to accurately determine the energy release contribution to the material damage process. The energy release in nonlinear fracture mechanical process is consumed in several different dissipation processes, e.g. surface separation, dislocation movement and hence plastic dissipation, heat conduction, and may be even phase transformation, etc. In fact, both Kfouri [18] and Wnuk [31] have studied energy release caused by the extension of Dugdale-BCS cracks in a two-dimensional space. To incorporate those available results into the current formulation, an in-depth study may be needed to refine the damage models proposed here. A detailed companied mathematical exposition on cohesive damage model is reported in Li and Wang [21].

Acknowledgment

This work is supported by a research fund to Professor Shaofan Li by the committee on research in University of California at Berkeley, which is appreciated.

References

[1] G.I. Barenblatt, The formation of equilibrium cracks during brittle fracture, Journal of Applied Mathematics & Mechanics 23 (1959) 622–636, English translation from PMM 23 (1959) 434–444.
[2] G.I. Barenblatt, Mathematical Theory of Equilibrium Cracks in Brittle Fracture, Advances in Applied Mechanics, vol. 7, Academic Press, 1962, pp. 55–129.
[3] B. Budiansky, J.R. Rice, Conservation laws and energy release rates, Journal of Applied Mechanics 26 (1973) 201–203.
[4] B. Budiansky, R.J. O'Connell, Elastic moduli of a cracked solid, International Journal of Solids and Structures 12 (1976) 81–97.
[5] W.R. Chen, L.M. Keer, Fatigue crack growth in mixed mode loading, ASME Journal of Engineering Materials and Technology 113 (1991) 222–227.
[6] W.R. Chen, L.M. Keer, Mixed-mode fatigue crack propagation of penny-shaped cracks, ASME Journal of Engineering Materials and Technology 115 (1993) 365–372.
[7] D.S. Dugdale, Yielding of steel sheets containing slits, Journal of Mechanics and Physics of Solids 8 (1960) 100–104.

[8] J.D. Duva, J.W. Hutchinson, Constitutive potentials for dilutely voided nonlinear materials, Mechanics of Materials 3 (1984) 41–54.
[9] N. Fleck, Brittle fracture due to an array of microcracks, Proceedings of Royal Society of London Series A 432 (1991) 55–76.
[10] M. Gologanu, J.B. Leblond, J. Devaux, Recent extensions of Gurson's model for porous ductile metals, in: P. Suquet (Ed.), Continuum Micromechanics, Springer-Verlag, 1995, pp. 61–130.
[11] A.L. Gurson, Plastic flow and fracture behavior of ductile materials incorporating void nucleation, growth and interaction, Ph.D. Thesis, Brown University, RI, 1975.
[12] A.L. Gurson, Continuum theory of ductile rupture by void nucleation and growth: Part I. Yield criteria and flow rules for porous ductile materials, Journal of Engineering Materials and Technology 99 (1977) 2–15.
[13] R. Hill, Theory of mechanical properties of fiber-strengthened materials—III: Self-consistent model, Journal of the Mechanics and Physics of Solids 13 (1965) 189–198.
[14] R. Hill, A self-consistent mechanics of composite materials, Journal of the Mechanics and Physics of Solids 13 (1965) 213–222.
[15] J.W. Hutchinson, Crack tip shielding by micro-cracking in brittle solids, Acta Metallurgica 35 (1987) 1605–1619.
[16] M. Kachanov, Elastic solids with many cracks and related problems, in: J.W. Hutchinson, T. Wu (Eds.), Advances in Applied Mechanics, vol. 32, Academic Press, New York, 1994, pp. 259–445.
[17] L.M. Keer, T. Mura, Stationary crack and continuous distributions of dislocations, in: Proceedings of The First International Conference on Fracture, vol. 1, The Japanese Society for Strength and Fracture of Materials, 1965, pp. 99–115.
[18] A.P. Kfouri, Crack separation energy-rates for the DBCS model under biaxial modes of loading, Journal of Mechanics and Physics of Solids 27 (1979) 135–150.
[19] D. Krajcinovic, Damage Mechanics, Elsevier, Amsterdam–New York, 1996.
[20] F.A. McClintock, A criterion for ductile fracture by the growth of holes, ASME Journal of Applied Mechanics 35 (1968) 363–371.
[21] S.F. Li, G. Wang, On damage theory of a cohesive medium, International Journal of Engineering Science 42 (2004) 861–885.
[22] T. Mura, Micromechanics of Defects in Solids, Martinus Nijhoff Publishers, Dordrecht, 1987.
[23] S. Nemat-Nasser, M. Hori, Micromechanics: Overall Properties of Heterogeneous Materials, 2nd ed., Elsevier, Amsterdam–Lausanne–New York–Oxford, 1999.
[24] T. Pardoen, J.W. Hutchinson, An extended model for void growth and coalescence, Journal of the Mechanics and Physics of Solids 48 (2000) 2467–2512.
[25] J.R. Rice, A path independent integral and the approximate analysis of strain concentration by notches and cracks, ASME Journal of Applied Mechanics 35 (1968) 379–386.
[26] J.R. Rice, Mathematical analysis in the mechanics of fracture, in: H. Liebowitz (Ed.), Fracture: An Advanced Treatise, vol. 2, Academic Press, 1968, pp. 191–311.
[27] V. Tvergaard, Influence of voids on shear band instabilities under plane strain conditions, International Journal of Fracture 17 (1981) 389–407.
[28] V. Tvergaard, On localization in ductile materials containing voids, International Journal of Fracture 18 (1982) 237–251.
[29] V. Tvergaard, Material failure by void growth to coalescence, in: J.W. Hutchinson, T.Y. Wu (Eds.), Advances in Applied Mechanics, vol. 27, Academic Press, New York, 1990, pp. 83–151.
[30] V. Tvergaard, A. Needleman, Analysis of the cop-cone fracture in a round tensile bar, Acta Metallurgica 32 (1984) 157–169.
[31] M.P. Wnuk, Mathematical modeling of nonlinear phenomena in fracture mechanics, in: M.P. Wnuk (Ed.), Nonlinear Fracture Mechanics, Springer-Verlag, Wien–New York, 1990, pp. 359–451.